ChemComm

Accepted Manuscript

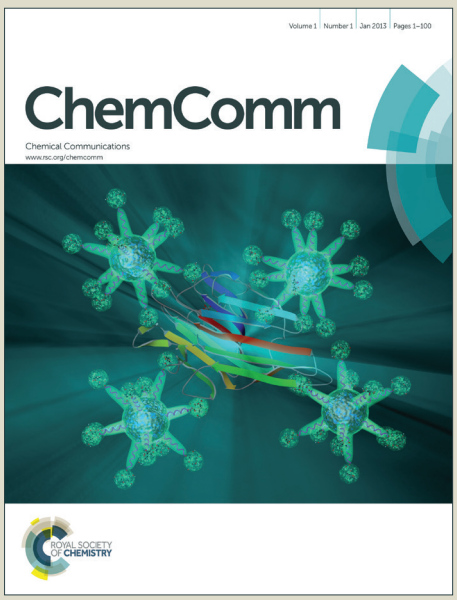

ROYAL SOCIETY OF CHEMISTRY

www.rsc.org/chemcomm

Cite this: DOI: 10.1039/c0xx00000x

www.rsc.org/xxxxxx

COMMUNTCATION

Plasmonic metal scattering immunoassay by total internal reflection scattering microscopy with nanoscale lateral resolution†

Seungah Lee,[a] Hyunung Yu[b] and Seong Ho Kang*[a]

Received (in XXX, XXX) Xth XXXXXXXXX 20XX, Accepted Xth XXXXXXXXX 20XX

DOI: 10.1039/b000000x

Immunoassays on nanopatterned chips through TIRS detection based on reconstructing three dimensional position provided a nanoscale accuracy of the lateral resolution by using the *z*-stage controller in the spatial range up to 10 nm. The method offers highly accurate and sensitive quantification giving the zeptomolar (~10^{-21} M) detection of proteins.

Traditionally, optical microscopy has been limited to two-dimensional imaging, and the possibility of measurement along the "vertical" direction has attracted little attention. Several imaging techniques have been proposed to determine the *z*-position of a single molecule or particle. Approaches[1] that use out-of-focus rings of the three-dimensional (3D) point-spread function (PSF) to infer the *z*-position are not capable of tracking quantum dots (QDs)[2] and pose several challenges for applications in live cell imaging. Many microscopic techniques have been developed for 3D localization in a single particle tracking field.[3-7] For example, 3D super-resolution fluorescence imaging has provided novel and meaningful information on *in vivo* ultra-structural imaging,[8] although studies based on super-resolution fluorescence-free imaging to the subdiffraction limit are still in their infancy.

So far, conventional immunoassays have been used in enzyme-linked immunosorbent assays (ELISA),[9] some electrochemical biosensors,[10,11] chemiluminescence immunoassays,[12,13] electrochemiluminescent immunoassays,[14] immunoradiometric assays,[15] bioluminescent immunoassays,[16] and fluorescent immunoassays.[17] Another approach that is useful for protein detection is the optical imaging of single molecules or particles under an optical microscope. The protein can be imaged with fluorescent-labeled antibodies using a fluorescence microscope.[18] Although fluorescence imaging enables the quantitative estimation of protein concentration in a sample by fluorescence intensity, it is a time consuming process that is hampered by the photobleaching of fluorescent dyes. To overcome this limitation, several methods of fluorescent-free optical imaging for biomolecules have been reported, including enhanced dark field,[19] differential interference contrast,[20] interferometric measurements,[21] and surface plasmon resonance imaging[22] by nanoparticle labeling. More recently, our lab reported on the use of a sandwich immunoassay on gold substrate using total internal reflection scattering (TIRS) microscopy.[23] Although optical imaging using TIRS of a plasmonic metal nanoparticle without fluorescent-labels has been obtained with sophisticated and clear images, immunoassays of infinitesimal samples in the *z*-direction based on TIRS microscopy with lateral super-resolution has not yet been reported.

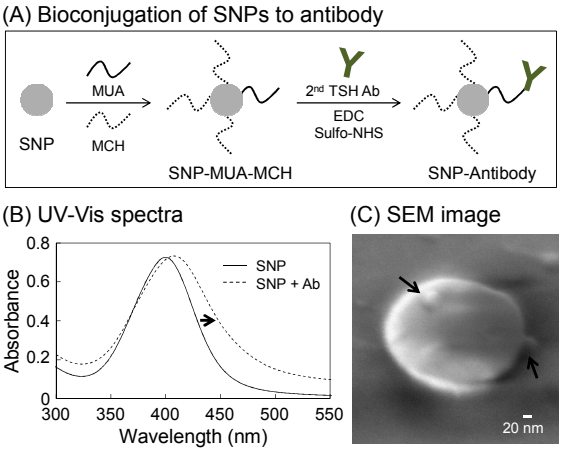

Fig. 1 (A) Schematic illustration for the modification of silver nanoparticles (SNPs) with 11-mercaptoundecanoic acid (MUA) and 6-mercapto-1-hexanol (MCH), and the conjugation with antibody. (B) UV-Vis spectra of 20 nm SNP-Ab dispersion (dotted line, λ_{max} = 408 nm) and 20 nm SNP solution (solid line, λ_{max} = 400 nm). (C) SEM images of 20 nm SNP-TSH antibody (Ab) on a 500 nm gold spot.

In the present study, we report for the first time a TIRS technique incorporating a *z*-nanopositioner for the accurate localization of molecules along the *z*-direction in immunoassays. TIRS is one of the strongest tools for high-contrast observation near solid-liquid interfaces. The intensity change of scattered light from plasmonic nanometals along the *z*-direction in evanescent field layers makes it possible to perform nanoparticle-scale detection of antibodies of infinitesimal samples (i.e., human thyroid-stimulating hormone, hTSH) on nanopatterned chips.

The first scattering signal occurred by the first metal-gold

[a] *Department of Applied Chemistry, Kyung Hee University, Yongin-si, Gyeonggi-do 446-701, Republic of Korea. E-mail: shkang@khu.ac.kr; Fax: +82 31 201 2340; Tel: +82 31 201 3349.*

[b] *Nanobio Fusion Research Center, Korea Research Institute of Standards and Science, Daejeon 305-600, Republic of Korea*

† Electronic Supplementary Information (ESI) available: Experimental section and supplementsary figures and movies. See DOI: 10.1039/b000000x/

nanopattern at a wavelength of 675 nm[19] and the secondary scattering signal occurred by silver nanoparticles (SNPs, 20 nm diameter) used as the secondary noble metal at a wavelength of 408 nm (Fig. 1B) on a gold-nanopatterned chip. The differences in wavelength of the scattering signals by these nanometals were selectively detected under specific illumination wavelengths (i.e., 405 nm and 671 nm lasers).

Total internal reflection (TIR) is one of the strongest tools for high-contrast observation near a glass surface. The principle of the height measurement method was based on the fact that the intensity of the evanescent field (I_z) decreases exponentially with perpendicular distance (z) from the TIR surface (circle in Fig. S1B).[24] This means that the intensity of the scattered light from a particle in this region strongly depends on its distance from the TIR surface. The evanescent field intensity decays exponentially with increases in distance from the interface according to the equation:

$$I_z = I_0 e^{-\frac{z}{d}} \qquad \text{Equation (1)}$$

where I_z represents the intensity at a perpendicular distance z from the interface, and I_o is the intensity at the interface. The characteristic penetration depth of the evanescent field $d(\theta)$ (θ; the incident angle of light) at λ_0, the wavelength of incident light in a vacuum, is given by:

$$d(\theta) = \frac{\lambda_0}{4\pi\sqrt{n_1^2 \sin^2\theta - n_2^2}} \qquad \text{Equation (2)}$$

If the size of the particle is much smaller than $d(\theta)$, then the total power of scattered light from the particle can also be written in the form: $exp(-z/d(\theta))$. When this is observed through an optical system, the intensity is multiplied by a factor of $psf(z)$ (point spread function). The observed intensity, therefore, is given by[25]

$$S(\theta, z) = S(\theta, 0) \cdot exp(-z/d(\theta)) \cdot H(z) \cdot psf(z) \qquad \text{Equation (3)}$$

where $S(\theta, 0)$ is the intensity of light scattered from the particle when it is closely attached to the TIR interface. $H(z)$ is a term representing the effect of interference between the particle and the surface. Equation (3) suggests that the scattering power depends not only on the height of the particle but also on the penetration depth of the evanescent field, $d(\theta)$: Therefore, by keeping $d(\theta)$ as the parameter and by varying it, we can control the scattered intensity from the particle. Note that $d(\theta)$ is a function of the incident angle. Thus, we keep the same penetration depth (d = 195 nm) by tuning the incident angle of 62° and 63° between two lasers (405 nm and 671 nm wavelength) to estimate the position in the z-direction by the scattering intensity of a plasmonic metal. We could calculate the position of the plasmonic metal without any previous knowledge of $H(z)$ and $psf(z)$ by measuring the intensity for two incident angles, which is the greatest advantage of this method.

In previous study, atomic force microscopy (AFM) was used to confirm the occurrence of immunoreactions.[19,20] The height of the 500-nm-diameter gold spot increased by ~40 nm after an immunoreaction with 71.4 aM of the TSH protein (Fig. S2 in ESI†). The scanning electron microscopy (SEM) image could also detect the location of a 20 nm SNP on a 500 nm gold spot, as shown by the arrows in Fig. 1C. However, measurements of the height difference using AFM, as shown in Fig. S2, can sometimes be in disagreement due to preprocessing or sample damage. The main limitation is that 2D single particle localization can only detect individual particles in a thin focal plan. Therefore, 3D single-nanometal locating, which captures the full spatial orientation of particles, is important for understanding immunoreactions by molecular orientation (i.e., antibody and antigen) on nanoarray chips in the evanescent field layer.

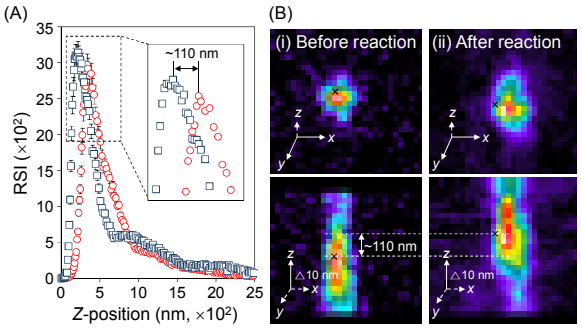

Fig. 2 (A) Plot of scattering intensity *vs* z-axis distance of a single spot before (blue) and after (red) immunoassay. (B) The axial (I_{xy}) and lateral (I_z) intensity distribution of the 3D point spread function (PSF) for TIRS imaging (i) before the immunoreaction and (ii) after the immunoreaction with the TSH antibody-silver nanoparticle. The black point (×) signifies the location of maximum scattering intensity.

Here, the SNP height z from the gold spot surface is varied in 10 nm steps for lateral resolution improvement. Gathering a number of 2D images at different z-positions is the most straightforward method for 3D single molecule/particle imaging and localizing on nanoarray chips. Fig. 2 shows the plot of scattering intensity *vs* z-axis distance of a single spot before (blue) and after (red) immunoassay. The relative scattering intensity (RSI) of the blue plot (for the gold spot) was measured with a 670/30 nm bandpass filter at 671 nm illumination, while the red plot (for the SNP) was measured with a 406/15 nm bandpass filter at 405 nm illumination. The difference of maximal scattering intensities was about 110 nm (Fig. 2A). In addition, the axial and lateral intensity distribution of the 3D point spread function (PSF) for TIRS imaging through "×" point (maxima RSI) could confirm the location of the SNP-TSH antibody on the gold spot after the immunoreaction in Fig. 2B. The maximum axial intensity (I_{xy}) of the gold spot before the immunoreaction occurred in the middle, while the maximum RSI of the gold spot after immunoreaction occurred on the left side of the intensity distribution. In the lateral intensity (I_z) distribution of 3D PSF, the location of the maximum RSI before/after the immunoreaction shows a clear distinction and difference of 110 nm, as shown in Fig. 2A (Fig. 2B, under). For these experiments, an important issue is to measure the location of the SNPs to the tens of nanometers after the sandwich immunoreaction on the gold spot. By simultaneously changing the z-position and detecting the scattered light, the silver nanoparticle's height from the TIR surface (on gold spot) could be calculated. An approach based on z-stack imaging for determining the 3D position of a point source has limitations in terms of its acquisition speed and the

achievable accuracy of location estimates, therefore posing a problem for imaging fast and highly complex 3D dynamics.[26] However, this limitation can be ignored in our work, as imaging antigen-antibody immunoreactions on a solid plate (i.e., a gold-nanopatterned chip) does not require high temporal precision.

In addition, we quantified TSH protein on a gold-nanopatterned chip based on plasmonic nanometal scattering by TIRS. The TSH concentration could be quantitatively calculated by the scattering intensity of the nano-metals (i.e., gold and silver) at different wavelengths. First, we selected signal and background regions with the same area. The sum of the TIRS intensities of the occupied pixels per single spot were corrected by background subtraction and the RSI was calculated. The scattered intensity obtained in this experiment is shown in Fig. 3. Line-sectional profiles of the scattering intensity (SI) based on the TIRS imaging in Fig. S3 shows a moderate increase with increasing hTSH concentration from 800 zM to 100 pM (Fig. 3A). The standard curve for serially diluted standard hTSH protein using TIRS shows a linear relationship in a wide range between 800 zM to 100 pM (correlation coefficient, R = 0.9900) under 405 nm laser illumination and with a 406 nm bandpass filter, as shown in Fig. 3B. A detection limit of 800 zM was achieved, which was below the guidelines recommended by the National Academy of Clinical Biochemistry (0.02 mIU/L = 118.7 fM).[27]

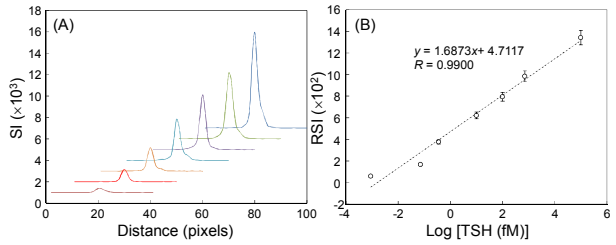

Fig. 3 The quantitative analysis of standard hTSH. (A) Line-sectional profiles of the scattering intensity (SI) and (B) the standard calibration curve by serial dilution concentrations (from 800 zM to 100 pM) of standard TSH. The relative scattering intensities (RSI) were corrected by background subtraction.

The use of light in optical microscopic measurements has traditionally been limited only to two-dimensional imaging, and the possibility of measurements along the "vertical" direction has attracted little attention. Especially, in immunoassay, increasing lateral spatial resolution provides detail information about nonspecific binding, molecular orientation, exact distance between target molecules and surface at the single molecule level. In this study, we first scaled the 3D image in the vertical direction to achieve the desired plasmonic metal's localization on a nanobiochip using TIRS with z-stacks microscopy. In the first step, a complete sandwich immunoassay based on the dependent wavelength with secondary-metal SNPs on first-metal gold-nanopatterned chips was proposed. In the second step, localization of the two metals could be measured by 3D image reconstruction in the evanescent field. Fluorescence-free imaging with subdiffraction-level resolution for the localization of the nanometals on the gold-nanopatterned chips was successfully achieved. Our TIRS detection system with a z-nanopositioner showed a spatial orientation of about ~110 nm, while the spatial resolution of conventional fluorescence microscopy is classically limited to about 200 – 300 nm in the lateral direction due to optical diffraction limitations. In addition, this technique supplied an opportunity to distinguish proximate neighbors with large differences in wavelength from native plasmonic nanometals through imaging in the lateral or axial direction. Finally, the quantitative analysis of low hTSH as a disease-related protein marker based on the sandwich immunoreaction on gold-nanopatterned chips was possible.

This research was supported by the Basic Science Research Program through the National Research Foundation of Korea (NRF) funded by the Ministry of Education, Science and Technology (2012R1A2A2A01013466).

Notes and references

1 M. Speidel, Jonas, A and E. L. Florin, *Opt. Lett.*, 2003, **28**, 69-71.
2 E. Toprak, H. Balci, B. H. Blehm and P. R. Selvin, *Nano Lett.*, 2007, **7**, 2043-2045.
3 Y. Katayama, O. Burkacky, M. Meyer, C. Brachle, E. Gratton and D. C. Lamb, *Chem. Phys. Chem.*, 2009, **10**, 2458-2464.
4 N. P. Wells, G. A. Lessard, P. M. Goodwin, M. E. Phipps, P. J. Cutler, D. S. Lidke, B. S. Wilson and J. H. Werner, *Nano Lett.*, 2010, **10**, 4732-4737.
5 A. Dupont and D. C. Lamb, *Nanoscale*, 2011, **3**, 4532-4541.
6 M. F. Juette, F. E. Rivera-Molina, D. K. Toomre and J. Bewersdorf, *Appl. Phys. Lett.*, 2013, **102**, 173702/1-173702/4.
7 B. van den Broek, B. Ashcroft, T. H. Oosterkamp and J. van Noort, *Nano Lett.*, 2013, **13**, 980-986.
8 C. G. Galbraith and J. A. Galbraith, *J. Cell Sci.*, 2011, **124**, 1607-1611.
9 H. Wang, X. Wu, P. Dong, C. Wang, J. Wang, Y. Liu and J. Chen, *Int. J. Electrochem. Sci.*, 2014, **9**, 12-21.
10 P. Kalimuthu, J. Tkac, U. Kappler, J. J. Davis and P. V. Bernhardt, *Anal. Chem.*, 2010, **82**, 7374-7379.
11 Y. Liu, N. Tuleouva, E. Ramanculov and A. Revzin, *Anal. Chem.*, 2010, **82**, 8131-8136.
12 Z. Lin, X. Wang, Z. J. Li, S. Q. Ren, G. N. Chen, X. T and J. M. Ying Lin, *Talanta*, 2008, **75**, 965-972.
13 Q. Xiao, H. Li and J. M. Lin, *Clin. Chim. Acta*, 2010, **411**, 1151-1153.
14 M. Sánchez-Carbayo, M. Mauri, R. Alfayate, C. Miralles and F. Soria, *Clin. Biochem.*, 1999, **32**, 395-403.
15 S. Mirapurkar, G. Samuel, S. D. Borkute and N. Sivaprasad, *J. Immunoassay Immunochem.*, 2012, **33**, 325-336.
16 L. A. Frank, A. I. Petunin and E. S. Vysotski, *Anal. Biochem.*, 2004, **325**, 240-246.
17 F. Wu, S. Han, T. Xu and Y. F. He, *Anal. Biochem.*, 2003, **314**, 87-96.
18 S. Lee and S. H. Kang, *Talanta*, 2012, **99**, 1030-1034.
19 S. Lee, H. Yu and S. H. Kang, *Chem. Commun.*, 2013, **49**, 8335-8337.
20 S. Lee and S. H. Kang, *Biosens. Bioelectron.*, 2014, **60**, 45-51.
21 M. W. Szkudlinski, V. Fremont, C. Ronin and B. D. Weintraub, *Physiol. Rev.*, 2002, **82**, 473-502.
22 N. Rodondi, W. P. den Elzen, D. C. Bauer, A. R. Cappola, S. Razvi, J. P. Walsh, B. O. Asvold, G. Iervasi, M. Imaizumi, T. H. Collet, A. Bremner, P. Maisonneuve, J. A. Sgarbi, K. T. Khaw, M. P. Vanderpump, A. B. Newman, J. Cornuz, J. A. Franklyn, R. G. Westendorp, E. Vittinghoff and J. Gussekloo, *JAMA.*, 2010, **304**, 1365-1374.
23 S. Lee, G. Park, S. K. Chakkarapani and S. H. Kang, *Biosens. Bioelectron.*, 2015, **63**, 444-449.
24 L. Helden, E. Eremina, N. Riefler, C. Hertlein, C. Bechinger, Y. Eremin and T. Wriedt, *Appl. Opt.*, 2006, **45**, 7299-7308.
25 T. Kurihara, R. Sugimoto, R. Kudo, S. Takahashi and K. Takamasu, *Int. J. Nanomanufacturing*, 2012, **8**, 419-431.
26 S. Ran, P. Prabhat, J. Chao, E. S. Ward and R. J. Ober, *Biophys. J.*, 2008, **95**, 6025-6043.
27 Z. Baloch, P. Carayon, B. Conte-Devolx, L. M. Demers, U. Feldt-Rasmussen, J. F. Henry, V. A. LiVosli, P. Niccoli-Sire, R. John, J. Ruf, P. P. Smyth, C. A. Spencer and J. R. Stockigt, *Thyroid*, 2003, **13**, 3-126.